MOLECULAR AND CELLULAR BIOLOGY, Feb. 2004, p. 1649–1654 Vol. 24, No. 4
0270-7306/04/$08.00+0 DOI: 10.1128/MCB.24.4.1649–1654.2004

Capn5 Is Expressed in a Subset of T Cells and Is Dispensable for Development

Tanna Franz, Lara Winckler, Thomas Boehm, and T. Neil Dear*

Department of Developmental Immunology, Max Planck Institute for Immunobiology, D-79108 Freiburg, Germany

Received 25 September 2003/Returned for modification 13 November 2003/Accepted 19 November 2003

The *Capn5* gene was inactivated by homologous recombination in ES cells that subsequently colonized the germ line of mice. The targeted mutation integrated a *lacZ* expression cassette into the *Capn5* gene, allowing the expression of *Capn5* mRNA to be examined in detail in heterozygous animals. Expression was observed in embryonic and newborn thymuses, in various epithelial tissues, and in tissues of the central nervous system. In the thymus, *Capn5* was expressed mainly in relatively immature CD25$^+$ embryonic thymocytes. Despite the numerous expression sites of *Capn5*, the majority of *Capn5*-null mice were viable and fertile and appeared healthy. Histopathological analysis did not reveal any differences between *Capn5*-null and wild-type mice. There were no defects in the major T- or B-cell populations in the thymus, spleen, bone marrow, or peritoneum, nor did apoptosis appear abnormal in *Capn5*-null T cells. There was no evidence for the development of autoimmune disease in *Capn5*-null animals. However, a small proportion of homozygous null offspring from heterozygous matings were runted and most often did not survive to adulthood.

Calpains are a family of cytosolic cysteine proteases. CAPN1 and CAPN2, which are dependent on micromolar and millimolar concentrations of Ca^{2+}, respectively, for their in vitro proteolytic activity, consist of an isoform-specific large (80-kDa) subunit and an invariant small (30-kDa) subunit termed CAPN4 (17). The large-subunit protein is conveniently divided into four domains, I to IV. The crystal structure of CAPN2 (15, 37) reveals that catalytic domain II consists of two subdomains, IIa and IIb, which are reoriented upon Ca^{2+} binding to generate the protease active site. Domain III has some structural similarity to the C_2 domain, which is known to bind Ca^{2+} (29). The crystal structure of the small subunit, which associates with domain IV, demonstrates the presence of five Ca^{2+}-binding EF hand motifs in the C-terminal region of calpain (3, 21).

The calpain family consists of 13 different large-subunit genes (9). CAPN1, -2, -8, -9, -11, -12, and -14 conform to the classic four-domain structure described above (11, 12, 19, 34), whereas CAPN3 contains two large insertions (33). CAPN5, -6, -7, and -10 possess alternative C-terminal domains (4, 10, 13), and CAPN13 lacks domain IV altogether (9). In CAPN5, this domain, termed domain T, possesses homology to the C_2 domain of phospholipases, as does domain N of CAPN7 (32; T. N. Dear and T. Boehm, unpublished data). Thus, these proteins, although lacking EF hand motifs, may still bind Ca^{2+}. In addition, CAPN6 lacks amino acids that are considered to be essential for the cysteine protease active site (10).

Although a great deal of biochemical information on calpains has been accumulated, their physiological role is unclear. They function by limited cleavage of a variety of substrates (5) and have been implicated in a variety of processes, including apoptosis (38), cell division (24), modulation of integrin-cytoskeleton interactions (31), and synaptic plasticity (6). They have been associated with numerous pathological conditions, such as Alzheimer's disease, cataracts, demyelination, cardiac ischemia, inflammation, and traumatic brain injury (for reviews, see references 5, 35, and 39). In humans, mutations in *CAPN3* are responsible for limb girdle muscular dystrophy type 2A (27). A single nucleotide polymorphism in intron 3 of *CAPN10* is associated with type 2 diabetes mellitus (14).

Calpain activity is also associated with apoptosis in a variety of systems. In neurons, for example, similarities in substrate specificity and mechanisms of activation between calpains and caspases have been noted (38). The protein p25, which accumulates in the brains of patients with Alzheimer's disease and leads to neuronal apoptosis, is cleaved from p35 by both CAPN1 and CAPN2 (18, 20). Caspase 12, which is required for amyloid-β neurotoxicity (26), can be activated by calpain (25).

Inactivation of specific calpain genes by homologous recombination is one potential method of gaining insight into calpain function. Disruption of mouse *Capn4* results in embryonic lethality (1), while its inactivation in 3T3 cells leads to transformation and tumorigenesis (22). Disruption of *Capn1* alters platelet function, but otherwise mice are viable and fertile (2). Inactivation of mouse *Capn3* generates a phenotype similar to human limb girdle muscular dystrophy type 2A and results in apoptosis of skeletal myofibers possibly due to altered accumulation and nuclear translocation of IκB and NF-κB (28). We have used gene targeting in ES cells to inactivate the *Capn5* gene.

MATERIALS AND METHODS

Mice. *Capn5*-null mice were maintained on a mixed 129/SvJ, C57BL/6J genetic background. For embryos, mice were mated in the evening and if a vaginal plug was observed the next morning, fertilization was assumed to have taken place at midnight.

Targeting strategy. Genomic clones for *Capn5* were obtained by screening a 129/SvJ genomic DNA library constructed in the cosmid vector pSuperCos (Stratagene, La Jolla, Calif.). The genomic organization of *Capn5* has been

* Corresponding author. Mailing address: Mary Lyon Centre, Medical Research Council, Harwell, Didcot OX11 0RD, United Kingdom. Phone: 44 1235 841104. Fax: 44 1235 841200. E-mail: n.dear@har.mrc.ac.uk.

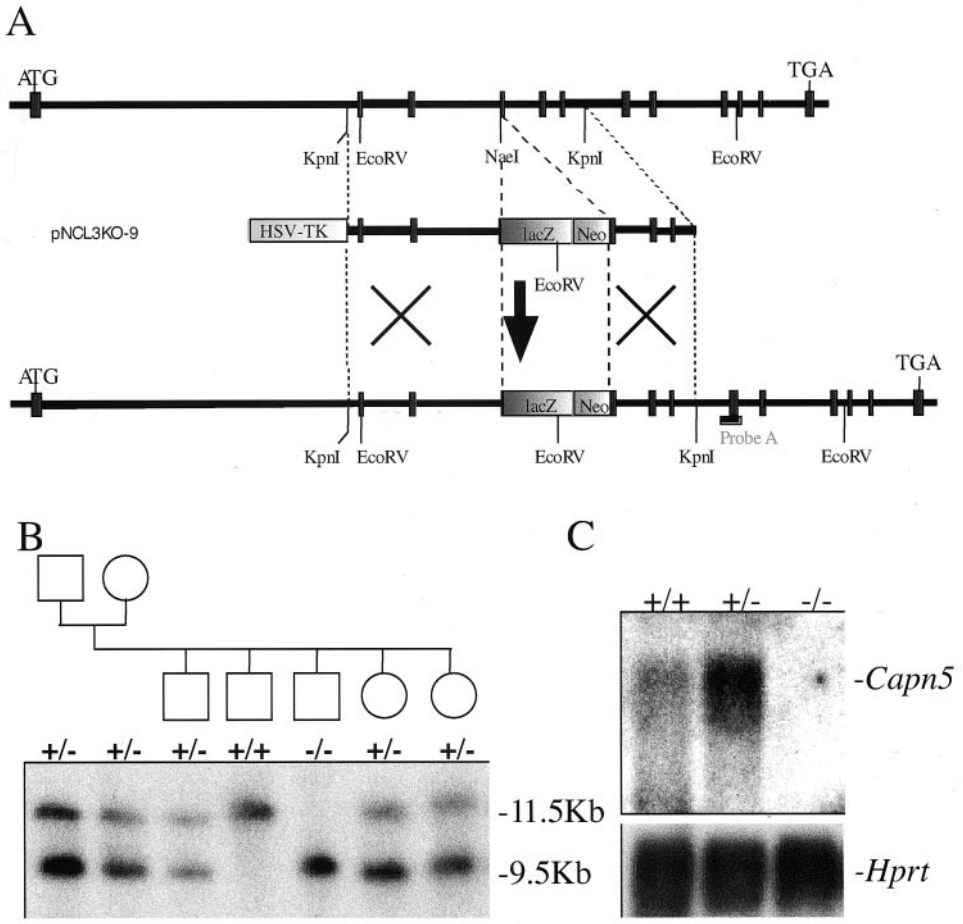

FIG. 1. Targeted disruption of the *Capn5* gene. (A) The targeting construct was made by inserting an IRES-*lacZ*-Neo cassette into the *Nae*I restriction site in exon 4 of *Capn5* genomic DNA. The linearized targeting construct and the endogenous genomic locus with relevant restriction enzyme sites are shown. The positions of the primers used for PCR analysis and the probe used for Southern blot analysis are indicated. (B) Southern blot analysis of *Eco*RV-digested DNAs from offspring of heterozygous matings hybridized with the ^{32}P-labeled probe. The 11.5- and 9.5-kb bands generated from the wild-type and knockout alleles are indicated. (C) Northern blot analysis of total RNAs from the brains of wild-type mice and mice heterozygous and homozygous for the targeted *Capn5* allele hybridized with a ^{32}P-labeled *Capn5* cDNA probe. The 2.3-kb *Capn5* RNA transcript present in the wild-type and heterozygous samples is indicated. The blot was rehybridized with an *Hprt* cDNA probe to confirm that equivalent levels of RNA had been loaded. HSV-TK, herpes simplex virus thymidine kinase.

published previously (23). A 7-kb *Kpn*I fragment encompassing exons 2 to 6 was subcloned into the vector pBluescript. An IRES-*lacZ*-MC1Neo cassette was inserted into the *Nae*I site located within exon 3, and a herpes simplex virus thymidine kinase cassette for negative selection was inserted downstream of the short arm of homology to create the targeting construct pNCL3KO-9.

Generation of *Capn5*-deficient mice. The targeting construct pNCL3KO-9 was linearized with *Not*I, and 25 μg was electroporated into 10^7 CJ7 ES cells. Selection proceeded in the presence of 400 μg of G418 per ml (active concentration) and 2 μM ganciclovir. After 9 days, colonies were picked, expanded, and analyzed by Southern blot analysis to identify targeted ES clones. The homologous targeting efficiency was 1 in 20. Positive clones were further analyzed to exclude any clones containing multiple insertions of the targeting vector. ES cells from two independent clones were injected into C57BL/6J blastocysts and largely agouti male chimeras were mated to C57BL/6J females. The resulting F_1 offspring were screened by Southern blot analysis of tail biopsy genomic DNA for germ line transmission of the targeted allele and intercrossed to generate homozygous null mice.

Genotyping. DNA was isolated by tail biopsy, digested with *Eco*RV, separated by electrophoresis in a 0.8% (wt/vol) agarose gel, and transferred to Hybond-N nylon membrane. The membrane was hybridized to a ^{32}P-labeled DNA probe corresponding to exon 7 of the *Capn5* genomic sequence.

FACS analysis. Before staining, cell suspensions from all organs were passed through a 40-μm cell strainer to remove residual connective tissue and cell clumps. For each staining, 2×10^6 cells were transferred into a tube and centrifuged at 1,000 × *g* for 5 min. The supernatant was discarded, the cells were resuspended in 10 μl of primary antibody solution by vortexing, covered with aluminum foil to prevent bleaching and quenching, and incubated for 15 min on ice. To remove unbound antibody, 2 ml of fluorescence-activated cell sorter (FACS) buffer was added and the tube was centrifuged at 1,000 × *g* for 5 min. The supernatant was discarded, and the cells were resuspended in 200 μl of FACS buffer (3% [vol/vol] fetal calf serum, 0.15% [wt/vol] sodium azide in phosphate-buffered saline [PBS]). At least 200,000 cells within the lymphocyte live gate were acquired with a FACScalibur (Becton Dickinson). The data were collected and analyzed with CellQuest. The antibodies were labeled as follows: anti-CD3–allophycocyanin; anti-CD25–phycoerythrin; anti-CD44–Red670. All antibodies were obtained from Pharmingen and used at a dilution of 1:50.

β-Galactosidase staining of tissues. Embryos or tissues were removed and fixed by incubating for 1 to 3 h in 4% (wt/vol) paraformaldehyde in PBS at 4°C with gentle shaking. The tissues were then washed briefly in PBS and incubated in staining solution (1 mg of 5-bromo-4-chloro-3-indolyl-β-D-galactopyranoside [X-Gal] per ml, 5 mM crystalline potassium ferricyanide, 5 mM potassium ferricyanide trihydrate, and 2 mM $MgCl_2$ in PBS) for up to 48 h. Staining was monitored and terminated at an appropriate time point by washing in PBS, followed by refixation for 16 h at 4°C.

Detection of β-galactosidase-positive cells by FACS analysis. Embryonic thymus tissue was isolated and disaggregated by being pushed through a sieve and

passed through a 40-μm cell strainer. A total of 200 μl of prewarmed staining solution (2 mM fluorescein di-β-D-galactopyranoside [FDG; Molecular Probes, Eugene, Oreg.], 4% [vol/vol] fetal calf serum, and 10 mM HEPES [pH 7.2] in PBS) was added, and the solution was incubated for 2 min at 37°C. FDG loading was then terminated by addition of 1.8 ml of ice-cold PBS containing 4% (vol/vol) fetal calf serum, 10 mM HEPES (pH 7.2), and 1 μg of propidium iodide per ml. Cells were then stained for other cell surface markers for FACS analysis. FDG-positive cells were monitored by emission at 512 nm by using excitation at 488 nm.

Northern blot RNA analysis. Total RNA was isolated from mouse tissues by the guanidine isothiocyanate method (7). Ten micrograms of total RNA was separated by electrophoresis in a 1.4% (wt/vol) agarose gel containing 2.2 M formaldehyde as previously described (30) and blotted to Hybond-N nylon membrane (Amersham) in accordance with the manufacturer's instructions. The blot was hybridized to a ^{32}P-labeled cDNA fragment corresponding to exons 7 to 15 of the *Capn5* cDNA sequence in Expresshyb hybridization solution (Clontech). Hybridization and high-stringency washing conditions were performed in accordance with the manufacturer's instructions. The blot was reprobed with an *Hprt* cDNA probe to confirm RNA loading.

RESULTS AND DISCUSSION

Generation of *Capn5*-null mice. The *Capn5* gene was disrupted by homologous recombination in ES cells. The targeting construct used contained an insertion of an IRES-*lacZ*-Neo cassette into exon 4 of *Capn5* (Fig. 1A). This strategy was chosen because even if a partial protein was produced from the targeted allele, the protease active site was likely to be disrupted, as the critical cysteine of the active site lies upstream of the insertion while the asparagine and histidine lie downstream. Additionally, the inclusion of the IRES-*lacZ* insertion allows the expression of *Capn5* in tissues to be examined by staining for β-galactosidase activity. Chimeric mice were generated from these ES cells. Four mice were generated, two of which demonstrated germ line transmission. Intercrossing of mice heterozygous for the targeted mutation generated *Capn5*-deficient mice. To differentiate the wild-type and targeted alleles, a ^{32}P-labeled probe corresponding to exon 7 and part of intron 6 was used, which detected 11.5- and 9.5-kb *Eco*RV fragments from the wild-type and targeted alleles, respectively. An example of a Southern blot analysis of DNAs from the weaned offspring of a mating between heterozygous mice is shown in Fig. 1B, indicating that mice homozygous for the targeted allele were viable.

To determine whether the targeted allele was being transcribed, total RNAs from the brains of wild-type and heterozygous and homozygous null mice were examined by Northern blot assay for *Capn5* RNA transcripts with a *Capn5* cDNA probe located downstream of the IRES-*lacZ* insertion. Brain tissue was chosen for analysis as, compared to other adult tissues, it expresses high levels of *Capn5* mRNA. There was no detectable *Capn5* mRNA in the homozygous null animals (Fig. 1C). A similar absence of *Capn5* mRNA was observed in liver RNA samples from homozygous null animals (data not shown). Thus, it appears that no complete *Capn5* mRNA, and therefore no protein, can be produced in such mice.

Analysis of *Capn5* expression in heterozygous knockout mice. The null allele contained an integrated *lacZ* gene such that β-galactosidase is produced in cells normally expressing *Capn5*. This allowed a detailed examination of the expression pattern of *Capn5* by staining of tissues from heterozygous mice for β-galactosidase activity. By using in situ analysis, we previously found *Capn5* mRNA to be expressed in the developing thymus and dorsal root ganglia (8). The *Capn5*^{lacZ} allele was also expressed in these tissues (Fig. 2A and B), confirming that this allele was functional. *lacZ* staining was strongest in the thymus between embryonic days 13.5 and 19. Expression was weaker in postnatal thymuses and undetectable in thymuses of 4-week-old mice (data not shown). Other expression sites identified included the outer epithelium of the stomach (Fig. 2C and D), the pons nuclei and other nuclei of the brain (Fig. 2E), the bladder epithelium (Fig. 2F), and the ganglia of the gut (Fig. 2G and H). Additionally, staining was also observed in the mucosal epithelium of the nostrils and the whisker barrels (data not shown).

In situ hybridization of a ^{33}P-labeled *Capn5* RNA probe to tissue sections confirmed the above-mentioned sites expressing

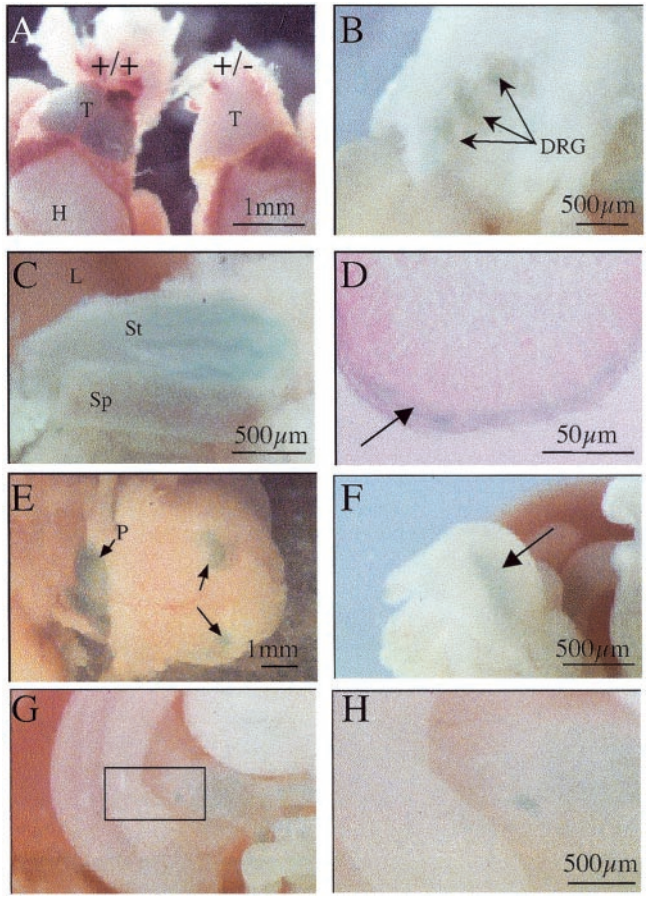

FIG. 2. Expression of the *Capn5*^{lacZ} allele during embryonic development. Postcoital day 14.5 embryos were removed and stained for β-galactosidase (*lacZ*) activity. Tissues were then dissected and photographed. (A) Comparative expression in the thymuses of *Capn5*$^{+/+}$ and *Capn5*$^{+/-}$ embryos. (B) Dorsal side of the neural tube of a *Capn5*$^{+/-}$ embryo showing expression in the dorsa root ganglia. (C) Expression in the epithelium of the stomach. (D) Histological section of the stomach stained for β-galactosidase expression and counterstained with hematoxylin and eosin. Expression is restricted to the epithelial cells (arrow). (E) Expression in the brain in the pons nuclei and nuclei in the forebrain region. (F) Expression in the bladder epithelium (arrow). (G) Expression in ganglia of the intestine. (H) Close-up of the boxed region in panel G. Abbreviations: DRG, dorsal root ganglia; L, liver; H, heart; P, pons nuclei; Sp, spleen; St, stomach; T, thymus.

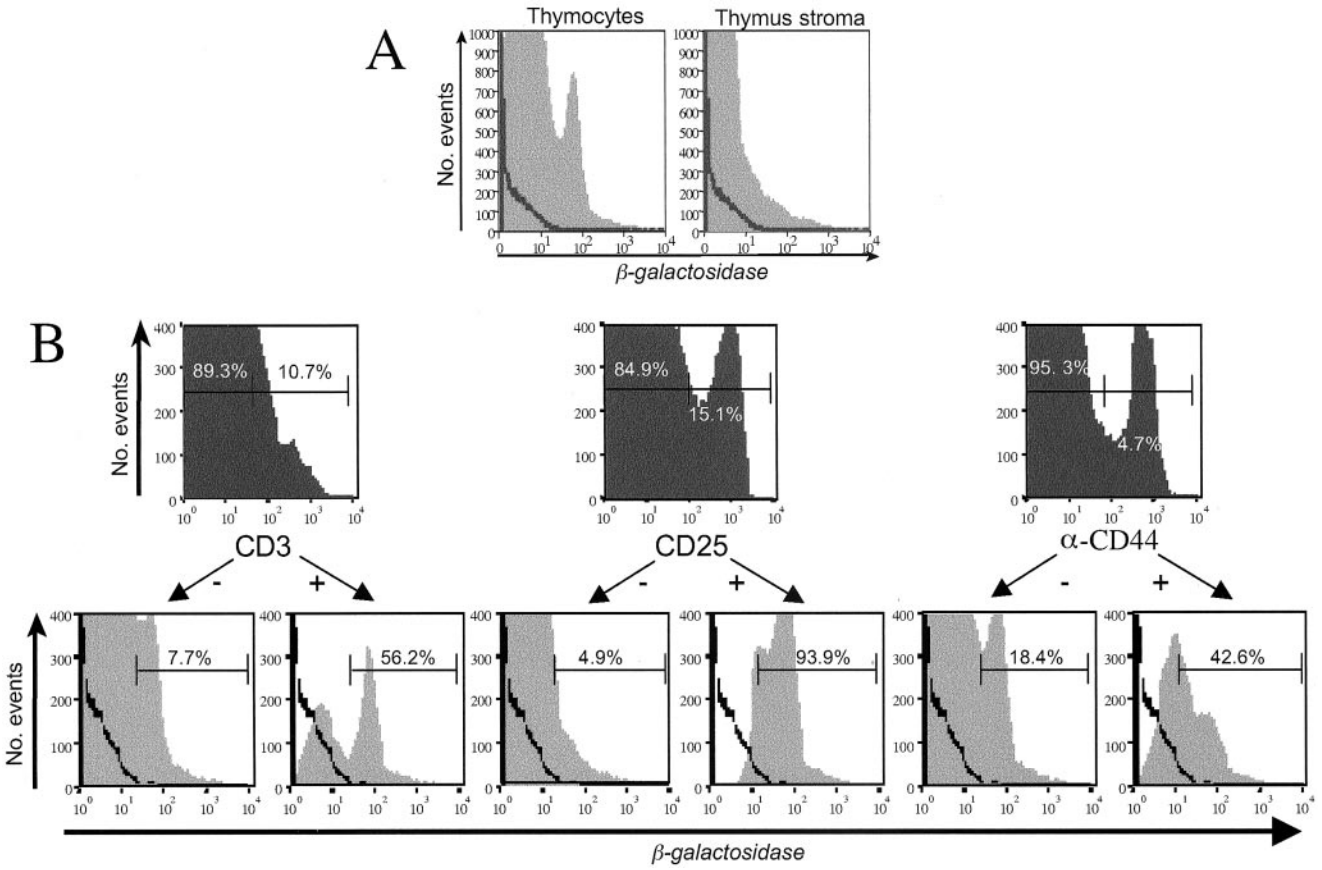

FIG. 3. Analysis of *Capn5*^{lacZ} allele expression in thymus cells. (A) Representative flow cytometric analysis of *Capn5*$^{+/-}$ thymocytes and stromal cells stained with FDG to detect β-galactosidase activity. (B) Representative flow cytometric analysis of cells stained with FDG and antibodies against CD3, CD25, and CD44. Cells staining positively or negatively for CD3, CD25, or CD44 (top) were gated and analyzed for expression of β-galactosidase (bottom).

Capn5 mRNA. In addition, several new sites were also uncovered that were not detected by β-galactosidase staining of heterozygous embryos, most likely because the expression was internal to the organ and thus masked in staining of whole organs. A common site was expression in epithelial cells. Expression was observed in the transitional epithelium of the afferent and efferent kidney tubules, the internal mucosa of the rectum, and the ependymal cells surrounding the central canal of the spinal cord, and weak expression was observed in the skin and the liver (data not shown). In adults, *Capn5* mRNA had been down-regulated in these tissues; exceptions were the pons nuclei and two unidentified nuclei of the forebrain. In situ hybridization also detected expression in the pyramid cells of the dorsal and ventral hippocampus (data not shown).

Expression of *Capn5* in T cells. As *Capn5* is prominently expressed in the embryonic and newborn thymus, we examined expression in this organ in greater detail. Thymus cells from newborn mice heterozygous for the targeted *Capn5*^{lacZ} allele were perfused with FDG, a substrate that is metabolized by β-galactosidase to a fluorescent compound that can be detected by FACS analysis. The *Capn5*^{lacZ} allele was expressed in about 15% of embryonic thymocytes with little expression in the stroma (Fig. 3A). FACS analysis was then performed with FDG in combination with various antibodies against thymocyte and stroma cell surface markers. None of the stromal subpopulations examined (dendritic cells, corticoepithelial cells, macrophages, and NK cells) expressed *Capn5*. In the thymocytes, there was no expression in the CD4, CD8, or γδTCR population (data not shown). Approximately half of the CD3-positive cells expressed *Capn5*. A similar proportion of CD44-positive cells expressed *Capn5* (Fig. 3B). All CD25$^+$ thymocytes were β-galactosidase positive, while CD25$^-$ thymocytes were negative (Fig. 3B). Thus, there is a strong correlation between the expression of CD25 and that of *Capn5*. This implies that *Capn5* is expressed in immature thymocytes. Clearly, however, there is some expression in more mature cells as some CD3$^+$ thymocytes expressed *Capn5*.

Despite this, detailed FACS analysis of subpopulations in the thymus, spleen, lymph nodes, peritoneal cavity, and blood of *Capn5*-null mice and wild-type littermate controls did not reveal any differences in the proportions of T cells positive for a variety of hematopoietic cell markers, including CD25, CD44, CD3, CD4, CD8, CD62L, CD69, TCRαβ, and TCRγδ (data not shown). A detailed analysis of the major immune cell populations of the spleen, thymus, bone marrow, peritoneum, lymph nodes, and peripheral blood was undertaken, but no differences between wild-type and *Capn5*-null mice were detected. The response of *Capn5*-null mice to typical T-depen-

dent and T-independent antigens was normal. As calpain activity has been associated with dexamethasone-induced apoptosis in thymocytes (36), such apoptosis was measured but no significant differences were observed between wild-type and *Capn5*-null thymocytes. Additionally, we tested whether *Capn5*-null mice were susceptible to induction of autoimmune diabetes by DNA vaccination with expression plasmids for insulin and GAD65 (16). Four-week-old mice were vaccinated at days 1 and 7 and observed for 4.5 months. No changes in blood glucose levels were observed between wild-type and *Capn5*-null mice. Furthermore, no other signs of autoimmunity, such as lymphocytic infiltrations in the salivary glands, adrenal glands, or liver, were observed.

***Capn5*-null mice exhibit reduced viability.** *Capn5*-null mice appeared normal. There were no obvious abnormalities in behavior, morphology, or development. There were no differences in β-galactosidase staining in heterozygous versus nullizygous embryos, suggesting that no major cell population is lost. We compared the distribution of genotypes in newborn litters of heterozygous matings. Examination of 17 litters (n = 120 pups) of $Capn5^{+/-} \times Capn5^{+/-}$ matings showed that the distribution of genotypes conformed to Mendelian expectations, with 37 (31%) $Capn5^{+/+}$, 54 (45%) $Capn5^{+/-}$, and 29 (24%) $Capn5^{-/-}$ mice ($P = 0.3$). It was notable, however, that a small number of pups from heterozygous matings (18 out of 418 pups = 4.3%) were severely runted at birth and most died by 3 weeks of age with a few surviving to 7 or 8 weeks of age (data not shown). DNA was obtained from nine of these runts, and all but one were homozygous for the *Capn5* null mutation; the other mouse was heterozygous. As homozygous *Capn5*-null mice were viable and fertile, matings were established between homozygous null animals. The proportion of runted offspring increased to 9.6% in such matings (10 out of 104 pups). As all offspring from such matings were homozygous for the null mutation, this increase in runted offspring further suggested that homozygosity for the *Capn5*-null mutation contributed to the runting observed. Of the 10 runted mice obtained from these matings, 1 male and 1 female mouse survived to adulthood and although runted appeared otherwise fit. No offspring were obtained from the male, but the female was fertile and $Capn5^{-/-}$ pups obtained from this female appeared healthy, were of a normal size, and grew at a normal rate. The mutation was bred into the C57BL/6J strain by six generations of backcrossing. When heterozygous animals in this background were intercrossed, no runted pups were observed among homozygous offspring.

Conclusions. In summary, *Capn5*-deficient mice do not suffer from striking abnormalities affecting any of the known expression sites. The genetic background appears to influence the phenotype, with runting and premature death resulting in a small proportion of animals. The calpain gene family is large, with possibly 13 large-subunit isoforms (9), and it may be that functional redundancy accounts for the lack of a phenotype in *Capn5*-null mice. Characterization of mutant mice carrying various combinations of calpain knockout alleles may assist in determining the role of each gene. Alternatively, the changes in *Capn5*-deficient mice may be subtle, affecting processes that have not yet been investigated, or may only be manifested upon a specific challenge. Furthermore, as the targeted modification of the *Capn5* gene results in a truncated protein, the possibility cannot be excluded that this protein retains some functional activity of sorts, thus acting as a hypomorphic rather than a nullimorphic allele.

ACKNOWLEDGMENTS

This work was partially supported by a grant from BASF, Ludwigshafen, Germany.

We thank Benoit Kanzler for blastocyst injection of ES cells and Melanie Hunn for technical assistance.

REFERENCES

1. **Arthur, J. S., J. S. Elce, C. Hegadorn, K. Williams, and P. A. Greer.** 2000. Disruption of the murine calpain small subunit gene, Capn4: calpain is essential for embryonic development but not for cell growth and division. Mol. Cell. Biol. **20:**4474–4481.
2. **Azam, M., S. S. Andrabi, K. E. Sahr, L. Kamath, A. Kuliopulos, and A. H. Chishti.** 2001. Disruption of the mouse μ-calpain gene reveals an essential role in platelet function. Mol. Cell. Biol. **21:**2213–2220.
3. **Blanchard, H., P. Grochulski, Y. Li, J. S. Arthur, P. L. Davies, J. S. Elce, and M. Cygler.** 1997. Structure of a calpain Ca^{2+}-binding domain reveals a novel EF-hand and Ca^{2+}-induced conformational changes. Nat. Struct. Biol. **4:**532–538.
4. **Braun, C., M. Engel, B. Theisinger, C. Welter, and M. Seifert.** 1999. CAPN 8: isolation of a new mouse calpain-isoenzyme. Biochem. Biophys. Res. Commun. **260:**671–675.
5. **Carafoli, E., and M. Molinari.** 1998. Calpain: a protease in search of a function? Biochem. Biophys. Res. Commun. **247:**193–203.
6. **Chan, S. L., and M. P. Mattson.** 1999. Caspase and calpain substrates: roles in synaptic plasticity and cell death. J. Neurosci. Res. **58:**167–190.
7. **Chomczynski, P., and N. Sacchi.** 1987. Single-step method of RNA isolation by acid guanidinium thiocyanate-phenol-chloroform extraction. Anal. Biochem. **162:**156–159.
8. **Dear, T. N., and T. Boehm.** 1999. Diverse mRNA expression patterns of the mouse calpain genes Capn5, Capn6 and Capn11 during development. Mech. Dev. **89:**201–209.
9. **Dear, T. N., and T. Boehm.** 2001. Identification and characterization of two novel calpain large subunit genes. Gene **274:**245–252.
10. **Dear, N., K. Matena, M. Vingron, and T. Boehm.** 1997. A new subfamily of vertebrate calpains lacking a calmodulin-like domain: implications for calpain regulation and evolution. Genomics **45:**175–184.
11. **Dear, T. N., A. Moller, and T. Boehm.** 1999. CAPN11: a calpain with high mRNA levels in testis and located on chromosome 6. Genomics **59:**243–247.
12. **Dear, T. N., N. T. Meier, M. Hunn, and T. Boehm.** 2000. Gene structure, chromosomal localization, and expression pattern of Capn12, a new member of the calpain large subunit gene family. Genomics **68:**152–160.
13. **Franz, T., M. Vingron, T. Boehm, and T. N. Dear.** 1999. Capn7: A highly divergent vertebrate calpain with a novel C-terminal domain. Mamm. Genome **10:**318–321.
14. **Horikawa, Y., et al.** 2000. Genetic variation in the gene encoding calpain-10 is associated with type 2 diabetes mellitus. Nat. Genet. **26:**163–175.
15. **Hosfield, C. M., J. S. Elce, P. L. Davies, and Z. Jia.** 1999. Crystal structure of calpain reveals the structural basis for Ca^{2+}-dependent protease activity and a novel mode of enzyme activation. EMBO J. **18:**6880–6889.
16. **Karges, W., K. Pechhold, S. Al Dahouk, I. Riegger, M. Rief, A. Wissmann, R. Schirmbeck, C. Barth, and B. O. Boehm.** 2002. Induction of autoimmune diabetes through insulin (but not GAD65) DNA vaccination in nonobese diabetic and in RIP-B7.1 mice. Diabetes **51:**3237–3244.
17. **Kawashima, S., M. Nomoto, M. Hayashi, M. Inomata, M. Nakamura, and K. Imahori.** 1984. Comparison of calcium-activated neutral proteases from skeletal muscle of rabbit and chicken. J. Biochem. (Tokyo) **95:**95–101.
18. **Kusakawa, G., T. Saito, R. Onuki, K. Ishiguro, T. Kishimoto, and S. Hisanaga.** 2000. Calpain-dependent proteolytic cleavage of the p35 cyclin-dependent kinase 5 activator to p25. J. Biol. Chem. **275:**17166–17172.
19. **Lee, H.-J., H. Sorimachi, S.-Y. Jeong, S. Ishiura, and K. Suzuki.** 1998. Molecular cloning and characterization of a novel tissue-specific calpain predominantly expressed in the digestive tract. Biol. Chem. **379:**175–183.
20. **Lee, M. S., Y. T. Kwon, M. Li, J. Peng, R. M. Friedlander, and L. H. Tsai.** 2000. Neurotoxicity induces cleavage of p35 to p25 by calpain. Nature **405:**360–364.
21. **Lin, G. D., D. Chattopadhyay, M. Maki, K. K. Wang, M. Carson, L. Jin, P. W. Yuen, E. Takano, M. Hatanaka, L. J. DeLucas, and S. V. Narayana.** 1997. Crystal structure of calcium bound domain VI of calpain at 1.9 Å resolution and its role in enzyme assembly, regulation, and inhibitor binding. Nat. Struct. Biol. **4:**539–547.
22. **Liu, K., L. Li, and S. Cohen.** 2000. Antisense RNA-mediated deficiency of the calpain protease, nCL-4, in NIH3T3 cells is associated with neoplastic transformation and tumourigenesis. J. Biol. Chem. **275:**31093–31098.
23. **Matena, K., T. Boehm, and N. Dear.** 1998. Genomic organization of mouse Capn5 and Capn6 genes confirms that they are a distinct calpain subfamily. Genomics **48:**117–120.

24. **Mellgren, R. L.** 1997. Evidence for participation of a calpain-like cysteine protease in cell cycle progression through late G_1 phase. Biochem. Biophys. Res. Commun. **236:**555–558.
25. **Nakagawa, T., and J. Yuan.** 2000. Cross-talk between two cysteine protease families. Activation of caspase-12 by calpain in apoptosis. J. Cell Biol. **150:** 887–894.
26. **Nakagawa, T., H. Zhu, N. Morishima, E. Li, J. Xu, B. A. Yankner, and J. Yuan.** 2000. Caspase-12 mediates endoplasmic-reticulum-specific apoptosis and cytotoxicity by amyloid-beta. Nature **403:**98–103.
27. **Richard, I., O. Broux, V. Allamand, F. Fougerousse, N. Chiannilkulchai, N. Bourg, L. Brenguier, C. Devaud, P. Pasturaud, C. Roudaut, D. Hillaire, M. Passos-Bueno, M. Zatz, J. A. Tischfield, M. Fardeau, C. E. Jackson, D. Cohen, and J. S. Beckmann.** 1995. Mutations in the proteolytic enzyme calpain 3 cause limb-girdle muscular dystrophy type 2A. Cell **81:**27–40.
28. **Richard, I., C. Roudaut, S. Marchand, S. Baghdiguian, M. Herasse, D. Stockholm, Y. Ono, L. Suel, N. Bourg, H. Sorimachi, G. Lefranc, M. Fardeau, A. Sebille, and J. S. Beckmann.** 2000. Loss of calpain 3 proteolytic activity leads to muscular dystrophy and to apoptosis-associated IκBα/nuclear factor κB pathway perturbation in mice. J. Cell Biol. **151:**1583–1590.
29. **Rizo, J., and T. C. Sudhof.** 1998. C2-domains, structure and function of a universal Ca^{2+}-binding domain. J. Biol. Chem. **273:**15879–15882.
30. **Sambrook, J., E. F. Fritsch, and T. Maniatis.** 1989. Molecular cloning: a laboratory manual, p. 7.43–7.45. Cold Spring Harbor Laboratory Press, Cold Spring Harbor, N.Y.
31. **Schoenwaelder, S. M., Y. Yuan, P. Cooray, H. H. Salem, and S. P. Jackson.** 1997. Calpain cleavage of focal adhesion proteins regulates the cytoskeletal attachment of integrin αIIbβ3 (platelet glycoprotein IIb/IIIa) and the cellular retraction of fibrin clots. J. Biol. Chem. **272:**1694–1702.
32. **Sokol, S. B., and P. E. Kuwabara.** 2000. Proteolysis in Caenorhabditis elegans sex determination: cleavage of TRA-2A by TRA-3. Genes Dev. **14:** 901–906.
33. **Sorimachi, H., S. Imajoh-Ohmi, Y. Emori, H. Kawasaki, S. Ohno, Y. Minami, and K. Suzuki.** 1989. Molecular cloning of a novel mammalian calcium-dependent protease distinct from both m- and mu-types. Specific expression of the mRNA in skeletal muscle. J. Biol. Chem. **264:**20106–20111.
34. **Sorimachi, H., S. Ishiura, and K. Suzuki.** 1993. A novel tissue-specific calpain species expressed predominantly in the stomach comprises two alternative splicing products with and without Ca^{2+}-binding domain. J. Biol. Chem. **268:**19476–19482.
35. **Sorimachi, H., S. Ishiura, and K. Suzuki.** 1997. Structure and physiological function of calpains. Biochem. J. **328:**721–732.
36. **Squier, M. K., A. C. Miller, A. M. Malkinson, and J. J. Cohen.** 1994. Calpain activation in apoptosis. J. Cell. Physiol. **159:**229–237.
37. **Strobl, S., C. Fernandez-Catalan, M. Braun, R. Huber, H. Masumoto, K. Nakagawa, A. Irie, H. Sorimachi, G. Bourenkow, H. Bartunik, K. Suzuki, and W. Bode.** 2000. The crystal structure of calcium-free human m-calpain suggests an electrostatic switch mechanism for activation by calcium. Proc. Natl. Acad. Sci. USA **97:**588–592.
38. **Wang, K. K.** 2000. Calpain and caspase: can you tell the difference? Trends Neurosci. **23:**20–26.
39. **Wang, K. K., and P. W. Yuen.** 1997. Development and therapeutic potential of calpain inhibitors. Adv. Pharmacol. **37:**117–152.